ACS APPLIED MATERIALS & INTERFACES

Research Article

www.acsami.org

Spray-On Polyaniline/Poly(acrylic acid) Electrodes with Enhanced Electrochemical Stability

Ju-Won Jeon, Se Ra Kwon, Fei Li, and Jodie L. Lutkenhaus*

Artie McFerrin Department of Chemical Engineering, Texas A&M University, College Station, Texas 77843, United States

Supporting Information

ABSTRACT: Polyaniline (PANI)-based electrodes are promising candidates for energy storage, but their cycle life remains poor. Recent work suggests that secondary interactions may enhance polyaniline's electrochemical stability and cycle life, but evidence to date is not conclusive. Here, we investigate spray-assisted layer-by-layer assemblies containing polyaniline nanofibers (PANI NFs) or conventional PANI and poly(acrylic acid) (PAA), which provides hydrogen bonding and electrostatic interactions. This spray-on approach may be suitable for the deposition of PANI onto a variety of surfaces. The effects of PANI type, PAA pH, and PAA molecular weight on the growth behavior, conductivity, and electrochemical performance are examined. It is shown that LbL films with PANI NFs, higher molecular weight PAA, and lower PAA pH yield the thickest films, whereas the thinnest films come from conventional PANI assembled under similar conditions. Electron microscopy imaging and density measurements show that LbL films containing PANI NFs are very porous, whereas those containing conventional PANI are very dense (0.28 vs 1.33 g/cm^3, respectively). The difference in density dramatically affects the electrochemical properties in terms of capacity and long-term cycling behavior. Upon extended cycling, PANI NFs alone rapidly lose their electrochemical activity. On the other hand, PANI NF-based LbL films exhibited somewhat enhanced stability, and PANI-based LbL films were exceptionally stable, maintaining 94.7% of their capacity after 1000 cycles when cycled up to 4.2 V vs Li/Li$^+$. These results show that secondary interactions from PAA enhance stability, as does the selection of PANI type and the electrode's density.

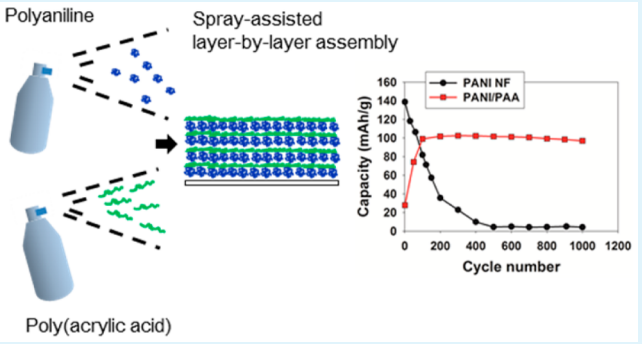

KEYWORDS: *polyaniline, poly(acrylic acid), layer-by-layer assembly, energy storage, batteries, spray*

INTRODUCTION

Polyaniline (PANI) is an intrinsically conductive polymer with unique redox activity, ease of synthesis, controllable conductivity, decent environmental stability, and low cost.[1−3] Owing to these properties, PANI has been investigated in a wide variety of applications including solar cells,[4] light-emitting devices,[5] catalysis,[6] sensors,[7] electrochromic devices,[8] and energy storage systems.[9] There is also an increasing interest in the deposition of PANI by various spraying methods,[10,11] since it simplifies application over large surfaces areas.

In energy storage systems, PANI has been studied as a battery electrode material since it is capable of storing charge by a unique dpoing−dedoping mechanism.[2,12−14] Its theoretical capacity is 294 mAh/g, which is higher than that of commercially available cathodes such as Li_xCoO_2 (theoretical capacity assuming x = 0.5:140 mAh/g) and Li_xFePO_4 (theoretical capacity assuming x = 1:170 mAh/g).[15,16] Furthermore, PANI has an electronic conductivity of 10−500 S/m, depending on the dopant.[17−20] However, in spite of its high theoretical capacity and excellent electrochemical properties, PANI's poor cycle life and electrochemical stability remains a considerable obstacle to its widespread use.[2,13,21,22] Most of its capacity is lost quite rapidly at relatively high potentials (>4 V vs Li/Li$^+$) in nonaqueous electrolytes, owing to side reactions with the electrolyte and irreversible oxidation of PANI to pernigraniline base.

Previously, we demonstrated enhanced electrochemical stability for PANI in the form of PANI:poly(2-acrylamido-2-methyl-1-propanesulfonic acid) (PAAMPSA).[2] Aniline was polymerized in the presence of PAAMPSA such that the two were intimately mingled and PAAMPSA acted as a dopant. Strong electrostatic interactions between the two stabilized PANI even in the pernigraniline salt form up to 4.5 V vs Li/Li$^+$.[2] Others have also reported enhanced PANI stability in hybrid electrodes.[23−26] Heat-treated PANI nanofiber/carboxylic acid functionalized multiwalled carbon nanotube (PANI NF/MWNT) layer-by-layer electrodes were stable up to 4.5 V vs Li/Li$^+$.[23,24] Single-walled carbon nanotube (SWCNT)/PANI aerogels synthesized also had excellent stability.[26] These reports suggest that secondary interactions (electrostatic, hydrogen-bonding) between PANI and an added species are responsible for PANI's enhanced electrochemical stability.

Received: August 12, 2015
Accepted: October 13, 2015
Published: October 13, 2015

DOI: 10.1021/acsami.5b07459
ACS Appl. Mater. Interfaces 2015, 7, 24150−24158

Layer-by-layer (LbL) assembly is an ideal manner to leverage secondary interactions in the pursuit of PANI's electrochemical stability in that it forms intimately mixed assemblies. In this method, complementary species, usually oppositely charged, are alternately adsorbed to a substrate.[27] The process may be repeated for n cycles to build up a film of n layer pairs. The properties of the resulting LbL films can be fine-tuned by controlling assembly conditions such as pH and ionic strength.[28,29] The coating deposits uniformly even onto objects of complex shape. The process may be conducted by simple immersion or by spraying.[30,31] The advantages of spray-assisted LbL assembly over dip-assisted LbL assembly includes shorter processing time, larger deposition area, and less cross-contamination.[11,32−34]

The LbL method has been recently implemented to build up hybrid PANI-containing electrodes for energy storage.[10−13,22−24,35,36] We specifically studied LbL assemblies of PANI and PAAMPSA, in which we found that these were far less stable than their template-polymerized PANI:PAAMPSA counterpart.[2,13] More recently, we have demonstrated the spray-assisted LbL assembly of electrodes containing polyaniline nanofibers and graphene oxide sheets[11] or V_2O_5.[10] These electrodes could be deposited over large surface areas in a fraction of the time as compared to dip-assisted LbL assembly. When cycled under modest conditions (up to 3.5 V vs Li/Li^+), the sprayed PANI/V_2O_5 exhibited reasonable stability, but higher voltages were desired to achieve enhanced capacities. In the pursuit of robust electroactive PANI-based coatings and electrodes, we desired to understand what contributes to PANI's electrochemical stability. These prior results suggest that secondary interactions play a role as does the extent of mixing, but evidence to date is not conclusive.

Here, we examine the assembly and electrochemical properites of PANI/poly(acrylic acid) (PAA) LbL films via spray-assisted LbL assembly. PAA is chosen as the complementary polyanion because it is inactive, thus allowing for observation of only PANI's electroactivity, and because carboxylic acid groups have shown some enhancement in PANI stability in past investigations.[23,24] We investigate the effect of PANI type, PAA pH, and PAA molecular weight on the LbL electrode's cycle thickness, roughness, density, electroactivity, and conductivity. Spray-assisted LbL assembly is selected as the preferred approach because of its relevance in spray-on batteries and capacitors.[37,38] Findings suggest that carboxylic acid groups indeed enhance stability, and that electrode density (or surface area) is also a critical factor.

EXPERIMENTAL SECTION

Materials. Poly(acrylic acid) (PAA, Mw = 100 000, 35% aqueous solution), emeraldine base polyaniline (Mw = 20 000), dimethylacetamide (DMAc), ammonium peroxydisulfate, aniline, lithium perchlorate, and propylene carbonate were obtained from Sigma-Aldrich. Linear polyethylenimine (PEI, Mw = 25 000), poly(acrylic acid) (Mw = 50 000, 25% aqueous solution), and poly(acrylic acid) (Mw = 1800, 63% aqueous solution) were purchased from Polysciences. Lithium ribbon was obtained from Alfa Aesar. Indium−tin oxide (ITO)-coated glass (<20 Ω) was purchased from Delta Technologies.

Layer-by-Layer Assembly. An emeraldine salt PANI dispersion was obtained by converting emeraldine base PANI according to previously reported methods.[13,39] First, 0.2 g of emeraldine base PANI was slowly added to 40 mL of DMAc. Subsequently, 12 h stirring and 10 h sonication were applied. The mixture was then vacuum-filtered (0.7 um glass filter) to remove large aggregates. The filtrate was poured into pH 3−3.5 deionized (DI) water at a ratio of 1:9 DMAc to water. Using HCl solution, the pH of the resulting mixture was lowered to 2.5. Another filtration step was employed before use. This procedure yielded a PANI dispersion of about 0.5 mg/mL emeraldine salt PANI in 1:9 DMAc and water.

PANI NFs were synthesized by a rapid mixing method.[12,40] Aniline (1.49 g) was dissolved in 50 mL of 1 M HCl. Ammonium peroxydisulfate (0.915 g) was dissoloved separately in 50 mL of 1 M HCl. Then, both solutions were purged with nitrogen for about 30 min. After purging, the ammonium peroxydisulfate solution was rapidly poured into the aniline solution at room temperature. The polymerization was carried out for 24 h. Then, the resulting solution was dialyzed against deionized water to remove impurities. The concentration was adjusted to 0.5 mg/mL by adding additional pH-adjusted deionized water. The final pH value was adjusted to 2.5 using HCl solution.

For LbL assembly, ITO-coated glass substrates were sonicated in dichloromethane, acetone, methanol, and deionized water for 15 min each. After washing, substrates were dried and subjected to oxygen plasma for 5 min. PANI NF (or PANI)/PAA films were assembled on ITO-coated glass substrates using an automated spray-assisted LbL system (Svaya Nanotechnologies). Before deposition of PANI and PAA, two layer pairs of LPEI/PAA were deposited using the 50 000 g/mol PAA.[10,41] First, 20 mM of LPEI solution (pH 4) was sprayed onto the substrates for 10 s, followed by spraying of pH 4 water for 10 s. Subsequently, 20 mM of PAA solution (pH 4) was sprayed for 10 s, followed by spraying of pH 4 water for 10 s. Once the two layer pairs of LPEI/PAA were deposited, PANI NF (or PANI)/PAA spray-assisted LbL films were assembled. The PANI NF (or PANI) dispersion was sprayed for 10 s, followed by 1 min of blow-drying with air. Similarly, PAA solution was sprayed for 10 s, and air was blown for 1 min. The procedure was repeated until the desired number of layer pairs was obtained. For all LbL films, the outermost layer was PANI.

Characterization. Film thickness was determined using profilometry (*P6*, KLA-Tencor). More than five different locations were measured for an average thickness. A quartz crystal microbalance (QCM, Inficon) was used to obtain the mass per area. The density was calculated with the combination of QCM and profilometry measurements. UV−vis absorption spectra were recored using a Hitachi U-4100 spectrometer. Scanning electron microscopy (SEM, JEOL JSM-7500F) was also used. Raman spectra were obtained using a 633 nm laser (Horiba Jobin Yvon). The electronic conductivity was measured using a four-point probe method (Keithley 2000 multimeter and 6221 DC and AC current source) with a probe spacing of 1.5875 mm at room temperature. Electrochemical testing (Solartron SI 1287) was performed using a three-electrode cell in a water-free, oxygen-free, argon-filled glovebox (MBraun). PANI NF (or PANI)/PAA LbL films on ITO-coated glass substrates were dried in air for at least 1 day before the measurement, and used as the working electrode. Li foil was used as counter and reference electrodes. As the electrolyte, 0.5 M $LiClO_4$ in propylene carbonate was used.

RESULTS AND DISCUSSION

Figure S1 shows scanning electron microscopy (SEM) images of drop-cast PANI and PANI NF dispersions. PANI NFs show well-defined fibers of diameter 40−80 nm. On the other hand, it was difficult to observe any notable features for drop-cast PANI. Both PANI and PANI NFs were in the conductive emeraldine salt form, identified using UV−vis spectroscopy (Figure S2). Both exhibited a long absorption tail (>800 nm) attributed to emeraldine salt's conductive nature.[13] The zeta potential of PANI and PANI NF dispersions were +30 and +35 mV, respectively. The pH of the adsorbing PANI dispersions was kept constant at pH 2.5 because of instability at more basic conditions. These results confirm the successful preparation of both dispersions and their suitability as the positively adsorbing species for LbL assembly.

In this study, we chose PAA, a weak polyacid with carboxylic acid functional groups, as the negatively adsorbing species. This

DOI: 10.1021/acsami.5b07459
ACS Appl. Mater. Interfaces 2015, 7, 24150−24158

selection is in contrast to our prior work with PAAMPSA,[13] which is a strong polyacid with sulfonic acid functional groups. As a weak polyacid with a reported solution pK_a of 5.5–6.5,[42−44] PAA is more sensitive to pH than PAAMPSA. Here, we investigate two pH values for PAA adsorption, pH 2.5 and 10. At the former, PAA exists mostly in its protonated form; at the latter, PAA is nearly completely ionized. Two different PAA molecular weights (1800 and 100 000 g/mol) were also investigated. The molecular structures of the emeraldine salt forms of PANI, PAA, and PAAMPSA are shown in Figure 1.

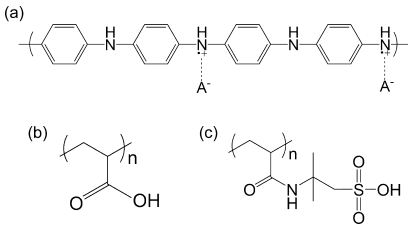

Figure 1. Molecular structures of (a) emeraldine salt polyaniline (PANI), (b) poly(acrylic acid) (PAA), and (c) poly(2-acrylamido-2-methyl-1-propanesulfonic acid) (PAAMPSA).

Layer-by-layer assembly was conducted by alternately spraying the PANI (or PANI NF) dispersion and PAA solution while blow-drying the sample between adsorption steps. The following systems were assembled: PANI NF/PAA-MW100,000-pH2.5, PANI NF/PAA-MW100,000-pH10.0, PANI NF/PAA-MW1,800-pH10.0, and PANI/PAA-MW100,000-pH2.5. The first and second numbers in this nomenclature stand for the molecular weight and pH of PAA, respectively. The color of the sample intensified with each subsequent deposition cycle (Figure S3). Profilometry was conducted to monitor the films' thickness and root-mean-square (RMS) roughness as a function of number of layer pairs (Figure 2). All films grew linearly with cycle thicknesses of 118.0 nm (PANI NF/PAA-MW100,000-pH2.5), 52.3 nm (PANI NF/PAA-MW100,000-pH10.0), 16.8 nm (PANI NF/PAA-MW1,800-pH10.0), and 5.1 nm (PANI/PAA-MW100,000-pH2.5) (Figure 2a and Table 1). Considering the diameter of the PANI NFs, the cycle thicknesses indicate that at least one layer of PANI NFs adsorb per cycle for the first two film types. For the last two film types, the cycle thickness was less than the PANI NF diameter,[22] which suggests patchy growth.

Reflecting upon the trends in cycle thickness, the molecular weight of PAA is a strong influence. PANI NF/PAA-Mw100,000-pH10 LbL films had a cycle thickness much greater than that of PANI NF/PAA-Mw1,800-pH10 (47.4 vs 14.4 nm/cycle). At 40.5 layer pairs, the PANI NF/PAA-Mw100,000-pH10 LbL film was almost 7 times thicker than PANI NF/PAA-Mw1,800-pH10 (1766 vs 260 nm). Several reports have investigated the effect of molecular weight on the growth profile of LbL films.[45−50] In most cases, using high molecular polyelectrolytes leads to larger cycle thicknesses, which is in good agreement with our results.[45,46,49,50] This is due to the fact that high molecular weight polyelectrolyte is simply larger than their low molecular weight polyelectrolyte analogue. Another possible factor is the packing of low molecular weight PAA into the porous PANI NF layers.

Besides molecular weight, the pH of the adsorbing PAA solution also influences cycle thickness. For example, the cycle

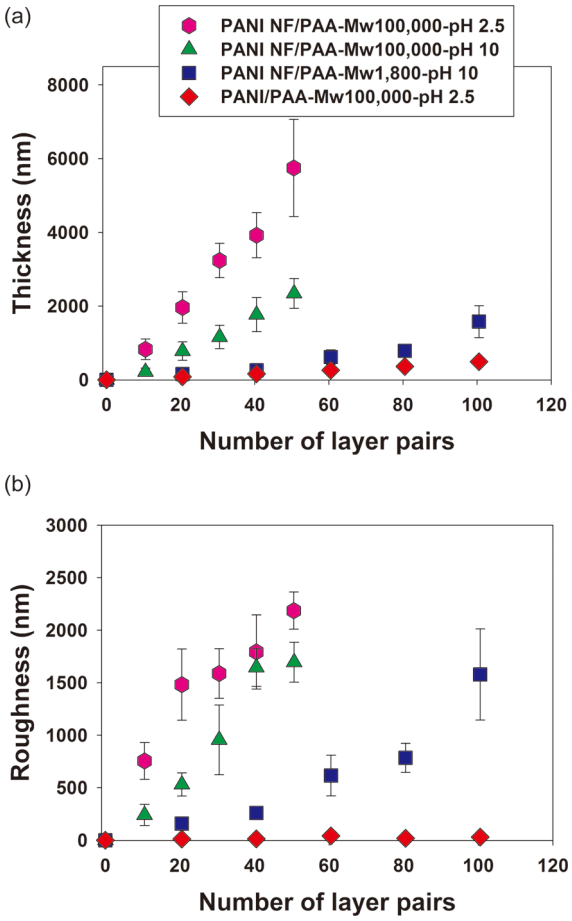

Figure 2. Thickness (a) and root-mean-square roughness (b) of LbL films versus the number of layer pairs deposited. Each data point represents the average and standard deviation of at least five profilometry measurements.

thickness of PANI NF/PAA-Mw100,000-pH2.5 was significantly higher than that of PANI NF/PAA-Mw100,000-pH10 (111.4 vs 47.4 nm/cycle). This is most probably due to the charge density of PAA in solution.[29,51] At pH 2.5, PAA chains are less ionized and possess more of a coiled conformation.[29] More PAA must adsorb to the positively charged preadsorbed PANI surface so as to compensate the surface charge, and the adsorbed PAA likely possesses many loops. At pH 10, PAA chains are fully charged and bear an extended chain conformation. Less PAA is required to reverse the surface charge during adsorption, and PAA adsorbs in a trainlike conformation rather than a loopy conformation.[29] These factors likely culminate in the reduced cycle thickness observed for pH 10.

Trends in roughness versus the number of layer pairs deposited tended to follow trends in thickness. PANI NF-based films were especially rough, with RMS roughness increasing beyond 2 μm in some cases as assembly proceeded. It is possible that the enhanced roughness affects adsorption by providing a higher surface area for species to adhere; this type of growth has been observed elsewhere for PANI-containing films and others.[29,52−55] This idea is supported in that the roughest films in Figure 2b have the largest cycle thickness in Figure 2a, and so forth. On the other hand, the PANI/PAA-Mw100,000-pH2.5 system had the smallest RMS roughness

DOI: 10.1021/acsami.5b07459
ACS Appl. Mater. Interfaces 2015, 7, 24150−24158

Table 1. Cycle Thickness, Density, and Conductivity of Various LbL Films Compared to PANI NFs

	PANI NF	PANI NF/PAA-Mw100,000-pH2.5	PANI NF/PAA-Mw100,000-pH10	PANI NF/PAA-Mw1,800-pH10	PANI/PAA-Mw100,000-pH2.5
thickness per cycle (nm)	n/a	118.0 (R^2 = 0.98)	52.3 (R^2 = 0.99)	16.8 (R^2 = 0.89)	5.1 (R^2 = 0.99)
density (g/cm^3)	0.24 ± 0.05	0.28 ± 0.03	0.27 ± 0.02	0.37 ± 0.06	1.33 ± 0.20
conductivity (S/m)	159.2	0.190	1.6×10^{-4}	1.3×10^{-4}	0.398

ranging from 10 to 40 nm and did not show any appreciable increase as assembly proceeded.

The density of the LbL films was obtained using a combination of QCM and profilometry. Density was calculated from the incremental mass and thickness deposited per adsorption step (Table 1). Spin-cast PANI NFs alone had a density of 0.23 g/cm^3, whereas all LbL films examined were denser. PANI NF/PAA-Mw100,000-pH2.5 and PANI NF/PAA-Mw100,000-pH10 both had a density of 0.28 g/cm^3, which suggests that the pH of PAA does not appreciably affect density. On the contrary, the molecular weight of PAA had a significant impact on film density; the density of PANI NF/PAA-Mw1,800-pH10 (0.37 g/cm^3) was much higher than that of PANI NF/PAA-Mw100,000-pH10 (0.28 g/cm^3). It is possible that low molecular weight PAA more easily penetrates and adsorbs into the porous LbL film, forming a more packed structure.[7] The type of PANI dispersion had the greatest impact on the film density. For example, PANI/PAA-Mw100,000-pH2.5 had a density of 1.33 g/cm^3, which is far higher than that of the other PANI NF-based films. Notably, the density of PANI/PAA-Mw100,000-pH2.5 is very similar to that of PANI itself (1.33 g/cm^3).[56]

Interestingly, when we tried to build up PANI NF/PAA-Mw100,000-pH10 LbL films using *dip*-assisted LbL assembly, it was difficult to grow the LbL films in a reliable and reproducible manner. In this process, when substrates are immersed in pH 10 PAA solution, the preadsorbed outermost PANI NF layer experiences a significant increase in pH, which changes its state from emeraldine salt to emeraldine base by dedoping. In the process, the preadsorbed PANI NFs lose their positive charge and the surface is rendered neutral,[57,58] precluding further LbL assembly. A similar phenomenon was also observed in poly(allyamine hydrochloride) (PAH)/PAA LbL films at extreme pH values.[29] However, when we use spray-assisted LbL assembly, PANI NF/PAA-Mw100,000-pH10 LbL films grow quite regularly. The critical difference is the time scale of the adsorption step (10 s for spraying vs 15 min for dipping). We believe that 10 s of spraying is long enough to adsorb PAA, but short enough to prevent the complete conversion of emeraldine salt to emeraldine base. This result implies that spray-assisted LbL assembly opens up new possibilities for growing films under more extreme conditions that are normally not suitable for dip-assisted LbL assembly.

SEM images of PANI NF/PAA-Mw100,000-pH2.5 and PANI/PAA-Mw100,000-pH2.5 are shown in Figure 3. The PANI NF/PAA LbL surface exhibited a porous fibrous structure, and a distinct PAA layer was not observed (Figure 3a,b). It is likely that PAA adsorbed onto the PANI NF surface but not in quantities so as to completely fill in open pores and voids. On the other hand, the PANI/PAA LbL surface was smooth and featureless (Figure 3c,d). These SEM images were consistent with the observed roughness and density for each respective LbL film.

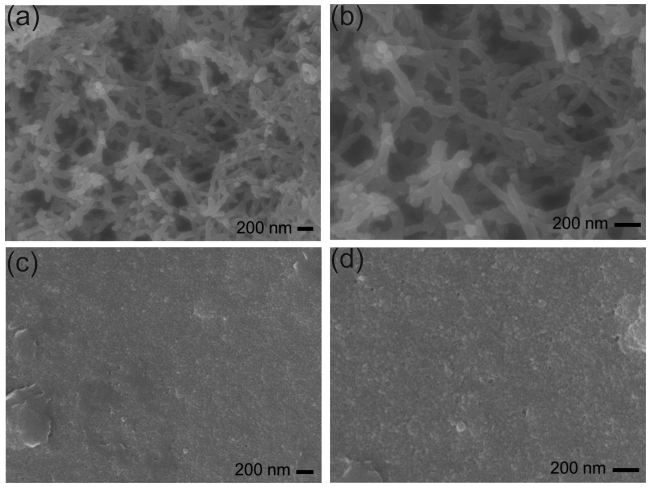

Figure 3. SEM images of (a, b) PANI NF/PAA-Mw100,000-pH2.5 and (c, d) PANI/PAA-Mw100,000-pH2.5 LbL films. The topmost layer is PANI.

The Raman spectra of PANI-NF, PAA, PANI/PAA-Mw100,000-pH2.5, and PANI-NF/PAA-Mw100,000-pH2.5 LbL films are shown in Figure S4. PAA homopolymer exhibits peaks at 1455, 1255, and 950 cm^{-1}, which can be ascribed to −COO−, C−H out of plane, and C−H bending, respectively.[59] For PANI, 1590, 1480, 1370, and 1168 cm^{-1} peaks were attributed to −C═C− stretching of quinoid,[23,60] C═N,[23] −C-N* radical,[23,60] and C−H in-plane groups,[61,62] respectively. For both LbL films, the Raman spectra were dominated by peak signatures from PANI, likely because PANI (or PANI NF) was the outermost layer.

The electronic conductivity of as-made LbL films was compared to that of drop-cast PANI NFs using a four-point probe under ambient conditions (Table 1). In all, cases the conductivity of the LbL films was lower than that of PANI NFs (159.2 S/m). LbL films assembled at pH 10 exhibited the lowest conductivity (ca. 10^{-4} S/m), which is a result of polyaniline's partial conversion to its insulating state in basic media. On the other hand, the conductivity of LbL films assembled at pH 2.5 was much higher at 0.190 and 0.398 S/m for PANI NF/PAA-Mw100,000-pH2.5 and PANI/PAA-Mw100,000-pH2.5, respectively. These results show that PAA's assembly pH heavily influences conductivity of the as-made LbL film, much more so than PAA molecular weight or PANI type.

The electrochemical properties of the LbL films were assessed in a nonaqueous three-electrode cell configuration using cyclic voltammetry. The electrolyte was 0.5 M $LiClO_4$ in propylene carbonate, and the counter and reference electrodes were separate lithium ribbons. The LbL film assembled on ITO served as the working electrode. To facilitate electrolyte penetration or electrode "conditioning", cyclic voltammetry was conducted for 50 cycles at 20 mV/s from 2 to 3.5 V vs Li/Li$^+$ (Figure 4a−c, Figure S5). Here, the maximum potential was

DOI: 10.1021/acsami.5b07459
ACS Appl. Mater. Interfaces 2015, 7, 24150−24158

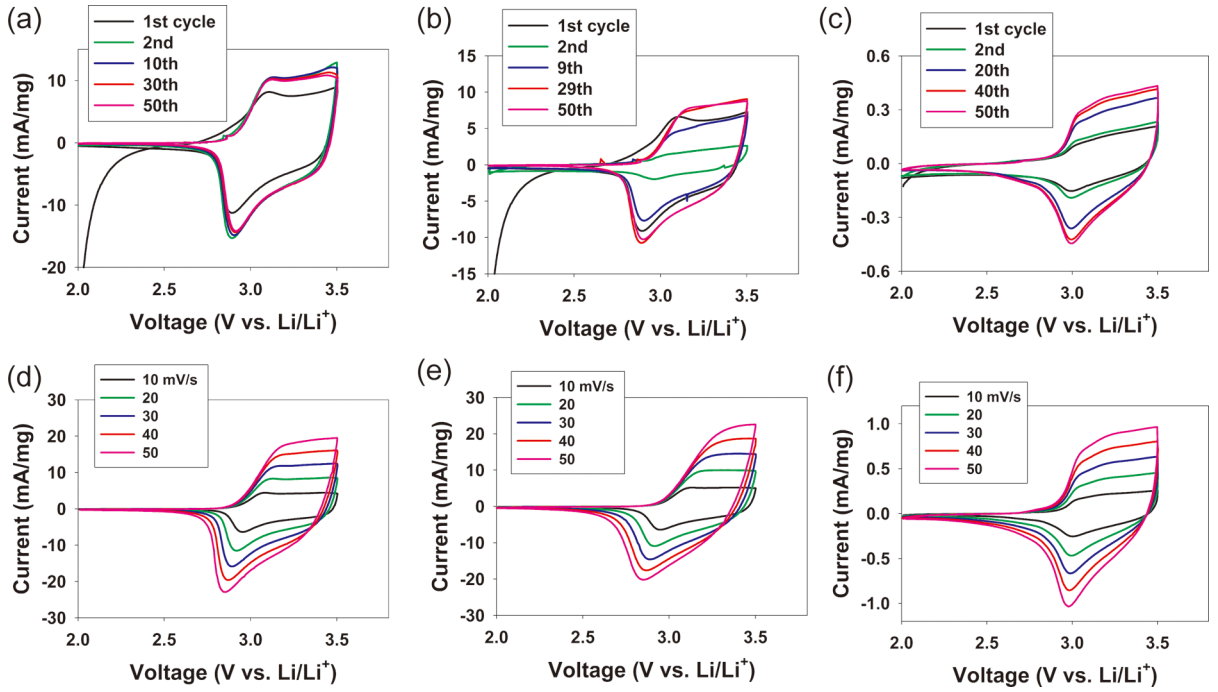

Figure 4. (a–c) Potentiodynamic cycling behavior of electrodes for 50 cycles at 20 mV/s. (d–f) Electrodes from (a–c) were then assessed using cyclic voltammetry at varying scan rates in a three-electrode cell. (a, d) = PANI NF; (b, e) = PANI NF/PAA-Mw100,000-pH10, and (c, f) = PANI/PAA-Mw100,000-pH2.5. The electrolyte was 0.5 M $LiClO_4$ in propylene carbonate, and the counter and reference electrodes were separate lithium ribbons. Electrode thickness ranged from 500 to 800 nm, and the current is reported on a basis of the mass deposited.

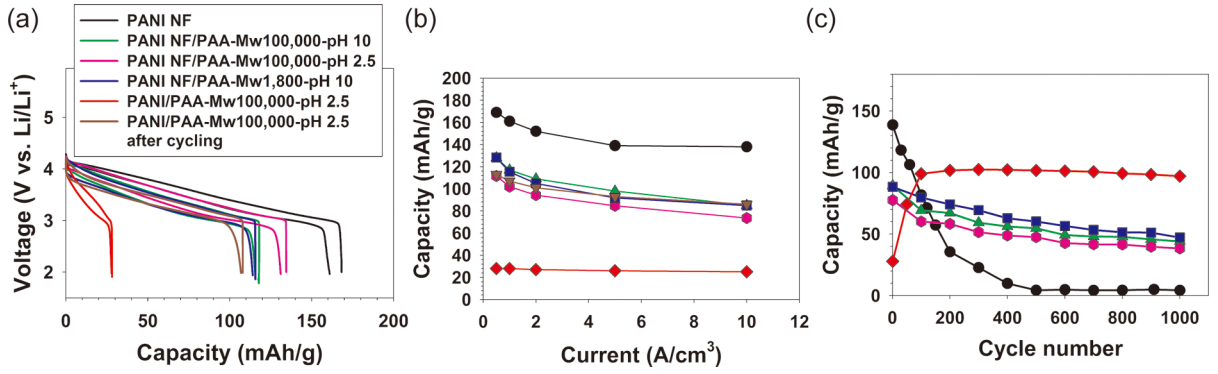

Figure 5. (a) Galvanostatic charge–discharge behavior at 1 A/cm^3 and (b) capacity vs current for various PANI-based electrodes. (c) Discharge capacity as measured from galvanostatic accelerated cycling at 5 A/cm^3. The electrolyte is 0.5 M $LiClO_4$ in propylene carbonate, and the counter and reference electrodes were separate lithium ribbons. Electrode thickness ranges from 500 to 800 nm, and the capacity is reported on a basis of the total mass deposited.

set to 3.5 V so as to avoid overoxidization of the electrode and to prevent degradation. The current is normalized by total mass of the deposited materials. Over the course of 50 cycles, cyclic voltammograms of spin-cast PANI NFs were steady with no changes in cycle shape (Figure 4a). On the other hand, both PANI NF/PAA-Mw100,000-pH10 and PANI/PAA-Mw100,000-pH2.5 exhibited a gradual increase and eventual stabilization in current over the 50 cycles. This behavior is consistent with gradual penetration of electrolyte into the electrode and activation of the electroactive materials. Electrodes presented in Figure 4a,b are both quite porous, yet electrolyte penetration influences only LbL electrodes with PAA. It is possible that PAA coats PANI NFs and thus needs some amount of cycling to fully imbibe the electrolyte and activate the PANI NFs. Further, the dense PANI-based LbL film (Figure 4c) also exhibits this effect, which is due either to its low porosity or to the presence of PAA. PANI NF/PAA-Mw1,800-pH10 and PANI NF/PAA-Mw100,000-pH2.5 also exhibit gradual increases in current during cycling, consistent with electrolyte penetration (Figure S5).

After electrode conditioning, cyclic voltammetry at various scan rates was carried out (Figure 4d–f). All electrodes show features characteristic of polyaniline. The anodic scan shows a capacitive plateau that appears above 3.0 V vs Li/Li^+ that is associated with the oxidation of leucoemeraldine base to emeraldine salt polyaniline. The cathodic scan shows a distinct peak at 2.8–3.0 V vs Li/Li^+, consistent with the reduction of emeraldine salt back to leucoemeraldine base polyaniline. There is no severe peak distortion, even up to 50 mV/s, and a plot of peak current versus scan rate was almost linear (Figure S6). These results imply that this is a surface-confined redox reaction.[13,63]

DOI: 10.1021/acsami.5b07459
ACS Appl. Mater. Interfaces 2015, 7, 24150–24158

Table 2. Gravimetric Capacities (mAh/g) of Various PANI-Based Electrodes at Varying Discharge Currents[a]

	0.5 A/cm^3	1 A/cm^3	2 A/cm^3	5 A/cm^3	10 A/cm^3
PANI NF (483 nm)	169	161	152	139	138
PANI NF/PAA-Mw1,800-pH10 (861 nm)	128	115	105	92	85
PANI NF/PAA-Mw100,000-pH10 (780 nm)	128	117	109	98	85
PANI NF/PAA-Mw100,000-pH2.5 (827 nm)	112	102	94	85	74
PANI/PAA-Mw100,000-pH2.5 (490 nm)	28	28	27	26	25
PANI/PAA-Mw100,000-pH2.5 (490 nm) *after 1000 cycles*	113	107	101	93	86

[a]Capacities are initial capacities, unless otherwise noted.

It is notable that the current associated with the PANI/PAA-Mw100,000-pH2.5 LbL electrode (511 nm) was low—about 20 times lower than that of a comparable drop-cast PANI NF electrode (755 nm thick). Although the PANI-based electrode is slightly thinner, this alone cannot explain the large difference in current. The decreased electroactivity is instead probably dominated by the dense electrode structure such that electrolyte does not readily move in and out of the electrode during cycling. The porous fibrous structure afforded by PANI NFs can facilitate transport of ions and electrolytes during the Faradaic redox reaction of PANI by providing void space, which can be beneficial for energy storage systems.[22,35,64]

To assess capacity, stability, and galavanostatic cycling behavior, conditioned electrodes were evaluated under constant-current conditions using the same three-electrode cell configuration as before (Figure 5a,b, Table 2). The volumetric capacities are shown in Table S1 for comparison. Here, cycling was carried out up to the highly oxidizing potential of 4.2 V vs Li/Li$^+$. As expected, PANI NFs had the highest capacity of 169 mAh/g at 0.5 A/cm^3 as compared to other LbL electrodes at the equivalent discharge current. PAA, which is not electroactive, dilutes the electroactive PANI and decreases the overall capacity. All PANI NF/PAA electrodes had similar capacities ranging from 112 to 128 mAh/g at 0.5 A/cm^3, regardless of PAA molecular weight or pH. Interestingly, PANI/PAA LbL films exhibited a very low capacity around 25 mAh/g even after conditioning. Again, the dense nature of these PANI/PAA films probably retards electrolyte penetration and lowers the overall electroactivity of the film. As discharge current increased, the capacity for all electrodes remained relatively constant, highlighting their good rate capability. These capacities are in line with the one-electron redox process for leucoemeraldine base/emeraldine salt conversion, having a theoretical capacity of 147 mAh/g. In comparing with other PANI-based LbL electrodes, PANI NF/PAA electrodes have a capacity lower than those of other PANI-based LbL electrodes consisting of two different electroactive species such as PANI NF/V_2O_5, PANI/reduced graphene oxide, and PANI NF/MWNT because of the presence of nonelectroactive PAA.[12,22,23,35] However, PANI NF/PAA electrodes bear higher capacities than other PANI-based LbL electrodes containing nonelectroactive PAAMPSA such as PANI/PAAMPSA, and PANI/PANI:PAAMPSA.[13]

Long-term galvanostatic cycling was performed at the relatively harsh conditions of 5 A/cm^3 from 2 to 4.2 V vs Li/Li$^+$ to investigate the electrochemical stability of the electrodes (Figure 5c). Under these conditions, it is expected that some amount of PANI should convert irreversibly to pernigraniline base.[2] Indeed, PANI NFs exhibited very poor cycling stability even though they had the highest initial capacity (Figure 5c). The PANI NF electrode lost 97% of its original capacity after 500 cycles. On the contrary, all PANI NF/PAA electrodes had significantly enhanced cycling stability. For example, PANI NF/PAA-Mw100,000-pH2.5 retained 61% of its initial capacity after 500 cycles, and 49% after 1000 cycles. No obvious variation in cycling behavior in regards to PAA molecular weight or pH was observed.

Among all electrodes investigated, the dense PANI/PAA-Mw100,000-pH2.5 electrode had the best cycling stability. The PANI/PAA-Mw100,000-pH2.5 electrode had a very small initial capacity of 26 mAh/g even though it was conditioned prior to galvanostatic cycling, indicative of incomplete electrolyte penetration in its initial state. Its capacity continuously increased up to 100 cycles and then held 94.7% of its maximum capacity up to 1000 cycles. It is possible that cycling at more extreme potentials (up to 4.2 V) further facilitiated penetration into this very dense electrode. The difference in cycling stability between PANI- and PANI NF/PAA-Mw100,000-pH2.5 is likely related to their extreme differences in density. It has been shown that porous high surface area electrodes may have compromised cycling stability possibly owing to the high surface area available for side reactions.[65,66] Here, particularly for the PANI/PAA LbL system, a nonporous structure may be preferable due to its significantly improved cycling stability even if additional conditioning is required to reach the maximum electroactivity.

The cycling stability for PANI/PAA LbL electrodes is quite impressive when compared to PANI/PAAMPSA LbL electrodes previously studied in our group.[13] For example, a PANI/PAAMPSA LbL electrode lost 93% of its original capacity after 1000 cycles even at moderate cycling conditions (1.5−3.5 V vs Li/Li$^+$).[13] On the other hand, template polymerized PANI:PAAMPSA possessed superior stability up to 4.5 V vs Li/Li$^+$.[2,13] Even though they possess the same components, the PANI/PAAMPSA LbL and PANI:PAAMPSA electrodes have fundamentally different structures. The former's structure is more akin to what we observe herein with PANI/PAA; however, the latter's structure is molecularly mixed, where aniline monomer is polymerized along PAAMPSA chains. As PANI is oxidized, it becomes positively charged, and PAAMPSA acts as a counterion to stabilize PANI's acquired positive charge.[2]

On the other hand, PANI/PAA LbL electrodes were able to maintain their capacity far longer than PANI/PAAMPSA LbL electrodes. In order explain this stark contrast of their oxidative stability, we considered the chemical structure and properties of PAA and PAAMPSA (Figure 1). PAAMPSA is a strong polyacid with sulfonic acid functional groups, and PAA is a weak polyacid with carboxylic acid functional groups.[2,58] The pK_a of PAAMPSA is substantially smaller than that of PAA (pK_a 2.4 vs 6.5, respectively), which means that PAAMPSA is far more acidic than PAA.[42,67] It is possible that PAA acts as a buffer, sharing protons with PANI during its reduction and oxidation as well as acting as a dopant. Electrostatic and

DOI: 10.1021/acsami.5b07459
ACS Appl. Mater. Interfaces 2015, 7, 24150−24158

hydrogen bonding interactions between PANI and PAA likely deter PANI's electrochemical degradation. Further, PAA may physically prevent the electrolyte from directly contacting PANI, thus further preventing side reactions. Interestingly, other PANI-containing LbL electrodes possessed greatly improved cycling stability when assembled with MWNTs and graphene sheets having carboxylic acid groups.[12,23]

CONCLUSION

PANI NF/PAA and PANI/PAA LbL electrodes were successfully assembled using spray-assisted LbL assembly. Film growth was strongly affected by PAA's assembly pH and molecular weight as well as the type of PANI. Cycle thickness decreased and film density increased as the PAA molecular weight decreased. Decreasing the PAA solution pH yielded films with larger cycle thicknesses, but density was not substantially affected. On the other hand, decreasing the PAA molecular weight yielded denser films with larger cycle thicknesses. LbL films containing PANI NFs were very porous, whereas those containing PANI were very dense. Electronic conductivity of the as-made films was most strongly controlled by PAA's assembly pH. All LbL electrodes investigated were electrochemically active, bearing PANI's distinctive electrochemistry. Most importantly, PANI's electrochemical stability was enhanced using weak polyacid PAA as a complementary species. Whereas PANI NFs lost 97% of their initial capacity after 500 cycles, a PANI/PAA LbL electrode retained 94.7% of its maximum capacity after 1000 cycles. This stability is thought to arise from secondary interactions between PANI and PAA, PAA as a physical barrier to direct contact with the electrolyte, and the decreased surface area.

More broadly, PANI has been investigated in a variety of applications including sensing, electrochromics, corrosion, organic electronics, and more. Beyond a presentation of the basic electrochemistry of spray-assisted LbL coatings, this work highlights a simple route to produce advanced functional PANI-based coatings in a spray-on approach, possibly suitable for application over large surfaces areas.

ASSOCIATED CONTENT

Supporting Information

The Supporting Information is available free of charge on the ACS Publications website at DOI: 10.1021/acsami.5b07459.

SEM images and UV−vis spectra of drop-cast PANI NFs and PANI. Digital images, Raman spectra, and cyclic voltammetry of various LbL films (PDF)

AUTHOR INFORMATION

Corresponding Author

*E-mail: jodie.lutkenhaus@tamu.edu.

Notes

The authors declare no competing financial interest.

ACKNOWLEDGMENTS

This work was supported in part by the Air Force Office of Scientific Research (Grant No. FA9550-13-1-0147) (spray-assisted LbL assembly), the Welch Foundation (A-1766) (stability), and 3M Non-Tenured Faculty Award. We thank the Materials Characterization Facility at TAMU.

REFERENCES

(1) Kang, E. T.; Neoh, K. G.; Tan, K. L. Polyaniline: A Polymer with Many Interesting Intrinsic Redox States. *Prog. Polym. Sci.* **1998**, *23*, 277−324.

(2) Jeon, J. W.; Ma, Y.; Mike, J. F.; Shao, L.; Balbuena, P. B.; Lutkenhaus, J. L. Oxidatively Stable Polyaniline:Polyacid Electrodes for Electrochemical Energy Storage. *Phys. Chem. Chem. Phys.* **2013**, *15*, 9654−9662.

(3) Shimano, J. Y.; MacDiarmid, A. G. Polyaniline, a Dynamic Block Copolymer: Key to Attaining its Intrinsic Conductivity? *Synth. Met.* **2001**, *123*, 251−262.

(4) Xiao, Y. M.; Lin, J. Y.; Wu, J. H.; Tai, S. Y.; Yue, G. T.; Lin, T. W. Dye-Sensitized Solar Cells with High-Performance Polyaniline/Multi-Wall Carbon Nanotube Counter Electrodes Electropolymerized by a Pulse Potentiostatic Technique. *J. Power Sources* **2013**, *233*, 320−325.

(5) Wang, H. L.; MacDiarmid, A. G.; Wang, Y. Z.; Gebier, D. D.; Epstein, A. J. Application of Polyaniline (Emeraldine Base, EB) in Polymer Light-Emitting Devices. *Synth. Met.* **1996**, *78*, 33−37.

(6) Das, B. C.; Iqbal, J. Polyaniline Supported Cobalt(II) Catalyst: Oxidation of Alkenes with Molecular Oxygen. *Tetrahedron Lett.* **1997**, *38*, 1235−1238.

(7) Athawale, A. A.; Chabukswar, V. V. Acrylic Acid-Doped Polyaniline Sensitive to Ammonia Vapors. *J. Appl. Polym. Sci.* **2001**, *79*, 1994−1998.

(8) DeLongchamp, D. M.; Hammond, P. T. Multiple-Color Electrochromism from Layer-by-Layer-Assembled Polyaniline/Prussian Blue Nanocomposite Thin Films. *Chem. Mater.* **2004**, *16*, 4799−4805.

(9) Niu, Z. Q.; Luan, P. S.; Shao, Q.; Dong, H. B.; Li, J. Z.; Chen, J.; Zhao, D.; Cai, L.; Zhou, W. Y.; Chen, X. D.; Xie, S. S. A "Skeleton/Skin" Strategy for Preparing Ultrathin Free-Standing Single-Walled Carbon Nanotube/Polyaniline Films for High Performance Supercapacitor Electrodes. *Energy Environ. Sci.* **2012**, *5*, 8726−8733.

(10) Shao, L.; Jeon, J.-W.; Lutkenhaus, J. L. Polyaniline Nanofiber/Vanadium Pentoxide Sprayed Layer-by-Layer Electrodes for Energy Storage. *J. Mater. Chem. A* **2014**, *2*, 14421−14428.

(11) Kwon, S. R.; Jeon, J.-W.; Lutkenhaus, J. L. Sprayable, Paintable Layer-by-Layer Polyaniline Nanofiber/Graphene Electrodes. *RSC Adv.* **2015**, *5*, 14994−15001.

(12) Jeon, J.-W.; Kwon, S. R.; Lutkenhaus, J. L. Polyaniline Nanofiber/Electrochemically Reduced Graphene Oxide Layer-by-Layer Electrodes for Electrochemical Energy Storage. *J. Mater. Chem. A* **2015**, *3*, 3757−3767.

(13) Jeon, J. W.; O'Neal, J.; Shao, L.; Lutkenhaus, J. L. Charge Storage in Polymer Acid-Doped Polyaniline-Based Layer-by-Layer Electrodes. *ACS Appl. Mater. Interfaces* **2013**, *5*, 10127−10136.

(14) Wu, Q.; Xu, Y. X.; Yao, Z. Y.; Liu, A. R.; Shi, G. Q. Supercapacitors Based on Flexible Graphene/Polyaniline Nanofiber Composite Films. *ACS Nano* **2010**, *4*, 1963−1970.

(15) Du Pasquier, A.; Plitz, I.; Menocal, S.; Amatucci, G. A Comparative Study of Li-ion Battery, Supercapacitor and Nonaqueous Asymmetric Hybrid Devices for Automotive Applications. *J. Power Sources* **2003**, *115*, 171−178.

(16) Dubarry, M.; Liaw, B. Y. Identify Capacity Fading Mechanism in a Commercial $LiFePO_4$ Cell. *J. Power Sources* **2009**, *194*, 541−549.

(17) Snook, G. A.; Kao, P.; Best, A. S. Conducting-Polymer-based Supercapacitor Devices and Electrodes. *J. Power Sources* **2011**, *196*, 1−12.

(18) Ryu, K. S.; Kim, K. M.; Park, N.-G.; Park, Y. J.; Chang, S. H. Symmetric Redox Supercapacitor with Conducting Polyaniline Electrodes. *J. Power Sources* **2002**, *103*, 305−309.

(19) Stejskal, J.; Gilbert, R. G. Polyaniline. Preparation of a Conducting Polymer (IUPAC technical report). *Pure Appl. Chem.* **2002**, *74*, 857−867.

(20) Ryu, K. S.; Kim, K. M.; Park, Y. J.; Park, N.-G.; Kang, M. G.; Chang, S. H. Redox Supercapacitor using Polyaniline Doped with Li Salt as Electrode. *Solid State Ionics* **2002**, *152−153*, 861−866.

(21) Song, R. Y.; Park, J. H.; Sivakkumar, S. R.; Kim, S. H.; Ko, J. M.; Park, D.-Y.; Jo, S. M.; Kim, D. Y. Supercapacitive Properties of

DOI: 10.1021/acsami.5b07459
ACS Appl. Mater. Interfaces 2015, 7, 24150−24158

Polyaniline/Nafion/hydrous RuO_2 Composite Electrodes. *J. Power Sources* **2007**, *166*, 297−301.
(22) Shao, L.; Jeon, J. W.; Lutkenhaus, J. L. Polyaniline/Vanadium Pentoxide Layer-by-Layer Electrodes for Energy Storage. *Chem. Mater.* **2012**, *24*, 181−189.
(23) Hyder, M. N.; Lee, S. W.; Cebeci, F. C.; Schmidt, D. J.; Shao-Horn, Y.; Hammond, P. T. Layer-by-Layer Assembled Polyaniline Nanofiber/Multiwall Carbon Nanotube Thin Film Electrodes for High-Power and High-Energy Storage Applications. *ACS Nano* **2011**, *5*, 8552−8561.
(24) Hyder, M. N.; Kavian, R.; Sultana, Z.; Saetia, K.; Chen, P. Y.; Lee, S. W.; Shao-Horn, Y.; Hammond, P. T. Vacuum-Assisted Layer-by-Layer Nanocomposites for Self-Standing 3D Mesoporous Electrodes. *Chem. Mater.* **2014**, *26*, 5310−5318.
(25) Tsutsumi, H.; Fukuzawa, S.; Ishikawa, M.; Morita, M.; Matsuda, Y. Polyaniline-Poly P-Styrenesulfonic acid-co-Methoxy-Oliga-(ethyleneglycol)acrylate Composite Electrode for All-Solid-State Rechargeable Lithium Battery. *J. Electrochem. Soc.* **1995**, *142*, L168−L170.
(26) Ge, D. T.; Yang, L. L.; Honglawan, A.; Li, J.; Yang, S. In Situ Synthesis of Hybrid Aerogels from Single-Walled Carbon Nanotubes and Polyaniline Nanoribbons as Free-Standing, Flexible Energy Storage Electrodes. *Chem. Mater.* **2014**, *26*, 1678−1685.
(27) Decher, G. Fuzzy Nanoassemblies: Toward Layered Polymeric Multicomposites. *Science* **1997**, *277*, 1232−1237.
(28) Buscher, K.; Graf, K.; Ahrens, H.; Helm, C. A. Influence of Adsorption Conditions on the Structure of Polyelectrolyte Multilayers. *Langmuir* **2002**, *18*, 3585−3591.
(29) Shiratori, S. S.; Rubner, M. F. pH-Dependent Thickness Behavior of Sequentially Adsorbed Layers of Weak Polyelectrolytes. *Macromolecules* **2000**, *33*, 4213−4219.
(30) Schaaf, P.; Voegel, J.-C.; Jierry, L.; Boulmedais, F. Spray-Assisted Polyelectrolyte Multilayer Buildup: from Step-by-Step to Single-Step Polyelectrolyte Film Constructions. *Adv. Mater.* **2012**, *24*, 1001−1016.
(31) Schlenoff, J. B.; Dubas, S. T.; Farhat, T. Sprayed Polyelectrolyte Multilayers. *Langmuir* **2000**, *16*, 9968−9969.
(32) Kim, S. Y.; Hong, J.; Kavian, R.; Lee, S. W.; Hyder, M. N.; Shao-Horn, Y.; Hammond, P. T. Rapid Fabrication of Thick Spray-Layer-by-Layer Carbon Nanotube Electrodes for High Power and Energy Devices. *Energy Environ. Sci.* **2013**, *6*, 888−897.
(33) Krogman, K. C.; Zacharia, N. S.; Schroeder, S.; Hammond, P. T. Automated Process for Improved Uniformity and Versatility of Layer-by-Layer Deposition. *Langmuir* **2007**, *23*, 3137−3141.
(34) Krogman, K. C.; Cohen, R. E.; Hammond, P. T.; Rubner, M. F.; Wang, B. N. Industrial-Scale Spray Layer-by-Layer Assembly for Production of Biomimetic Photonic Systems. *Bioinspiration Biomimetics* **2013**, *8*, 045005.
(35) Shao, L.; Jeon, J.-W.; Lutkenhaus, J. L. Porous Polyaniline Nanofiber/Vanadium Pentoxide Layer-by-Layer Electrodes for Energy Storage. *J. Mater. Chem. A* **2013**, *1*, 7648−7656.
(36) Mu, B.; Zhang, W. B.; Wang, A. Q. Template Synthesis of Graphene/Polyaniline Hybrid Hollow Microspheres as Electrode Materials for High-Performance Supercapacitor. *J. Nanopart. Res.* **2014**, *16*, 2432.
(37) Singh, N.; Galande, C.; Miranda, A.; Mathkar, A.; Gao, W.; Reddy, A. L. M.; Vlad, A.; Ajayan, P. M. Paintable Battery. *Sci. Rep.* **2012**, *2*, 481.
(38) Huang, C.; Grant, P. S. One-Step Spray Processing of High Power All-Solid-State Supercapacitors. *Sci. Rep.* **2013**, *3*, 2393.
(39) Cheung, J. H.; Stockton, W. B.; Rubner, M. F. Molecular-Level Processing of Conjugated Polymers 0.3. Layer-by-Layer Manipulation of Polyaniline via Electrostatic Interactions. *Macromolecules* **1997**, *30*, 2712−2716.
(40) Huang, J. X.; Kaner, R. B. Nanofiber Formation in the Chemical Polymerization of Aniline: A Mechanistic Study. *Angew. Chem., Int. Ed.* **2004**, *43*, 5817−5821.
(41) Abdelkader, R.; Amine, H.; Mohammed, B. Thermally Stable Forms of Pure Polyaniline Catalyzed by an Acid-Exchanged Montmorillonite Clay Called Maghnite-H^+ as an Effective Catalyst. *Int. J. Polym. Sci.* **2012**, *2012*, 846710.
(42) Choi, J.; Rubner, M. F. Influence of the Degree of Ionization on Weak Polyelectrolyte Multilayer Assembly. *Macromolecules* **2005**, *38*, 116−124.
(43) Bromberg, L. Properties of Aqueous Solutions and Gels of Poly(ethylene oxide)-b-Poly(propylene oxide)-b-Poly(ethylene oxide)-g-Poly(acrylic acid). *J. Phys. Chem. B* **1998**, *102*, 10736−10744.
(44) Philippova, O. E.; Hourdet, D.; Audebert, R.; Khokhlov, A. R. pH-Responsive Gels of Hydrophobically Modified Poly(acrylic acid). *Macromolecules* **1997**, *30*, 8278−8285.
(45) Jang, Y.; Seo, J.; Akgun, B.; Satija, S.; Char, K. Molecular Weight Dependence on the Disintegration of Spin-Assisted Weak Polyelectrolyte Multilayer Films. *Macromolecules* **2013**, *46*, 4580−4588.
(46) Xu, L.; Selin, V.; Zhuk, A.; Ankner, J. F.; Sukhishvili, S. A. Molecular Weight Dependence of Polymer Chain Mobility within Multilayer Films. *ACS Macro Lett.* **2013**, *2*, 865−868.
(47) Sun, B.; Jewell, C. M.; Fredin, N. J.; Lynn, D. M. Assembly of Multilayered Films using Well-Defined, End-Labeled Poly(acrylic acid): Influence of Molecular Weight on Exponential Growth in a Synthetic Weak Polyelectrolyte System. *Langmuir* **2007**, *23*, 8452−8459.
(48) Wong, J. E.; Diez-Pascual, A. M.; Richtering, W. Layer-by-Layer Assembly of Polyelectrolyte Multilayers on Thermoresponsive P(NiPAM-co-MAA) Microgel: Effect of Ionic Strength and Molecular Weight. *Macromolecules* **2009**, *42*, 1229−1238.
(49) Kujawa, P.; Moraille, P.; Sanchez, J.; Badia, A.; Winnik, F. M. Effect of Molecular Weight on the Exponential Growth and Morphology of Hyaluronan/Chitosan Multilayers: A Surface Plasmon Resonance Spectroscopy and Atomic Force Microscopy Investigation. *J. Am. Chem. Soc.* **2005**, *127*, 9224−9234.
(50) Borges, J.; Mano, J. F. Molecular Interactions Driving the Layer-by-Layer Assembly of Multilayers. *Chem. Rev.* **2014**, *114*, 8883−8942.
(51) Sun, W.; Zhou, S. X.; You, B.; Wu, L. M. A Facile Method for the Fabrication of Superhydrophobic Films with Multiresponsive and Reversibly Tunable Wettability. *J. Mater. Chem. A* **2013**, *1*, 3146−3154.
(52) Lvov, Y.; Ariga, K.; Onda, M.; Ichinose, I.; Kunitake, T. A Careful Examination of the Adsorption Step in the Alternate Layer-by-Layer Assembly of Linear Polyanion and Polycation. *Colloids Surf., A* **1999**, *146*, 337−346.
(53) McAloney, R. A.; Sinyor, M.; Dudnik, V.; Goh, M. C. Atomic Force Microscopy Studies of Salt Effects on Polyelectrolyte Multilayer Film Morphology. *Langmuir* **2001**, *17*, 6655−6663.
(54) Schoeler, B.; Poptoshev, E.; Caruso, F. Growth of Multilayer Films of Fixed and Variable Charge Density Polyelectrolytes: Effect of Mutual Charge and Secondary Interactions. *Macromolecules* **2003**, *36*, 5258−5264.
(55) DeLongchamp, D. M.; Kastantin, M.; Hammond, P. T. High-Contrast Electrochromism from Layer-by-Layer Polymer Films. *Chem. Mater.* **2003**, *15*, 1575−1586.
(56) Schnippering, M.; Powell, H. V.; Mackenzie, S. R.; Unwin, P. R. Real-Time Monitoring of Polyaniline Nanoparticle Formation on Surfaces. *J. Phys. Chem. C* **2009**, *113*, 20221−20227.
(57) Ryu, K. S.; Moon, B. W.; Joo, J.; Chang, S. H. Characterization of Highly Conducting Lithium Salt Doped Polyaniline Films Prepared from Polymer Solution. *Polymer* **2001**, *42*, 9355−9360.
(58) Tarver, J.; Yoo, J. E.; Dennes, T. J.; Schwartz, J.; Loo, Y. L. Polymer Acid Doped Polyaniline Is Electrochemically Stable Beyond pH 9. *Chem. Mater.* **2009**, *21*, 280−286.
(59) Murli, C.; Song, Y. Pressure-Induced Polymerization of Acrylic Acid: A Raman Spectroscopic Study. *J. Phys. Chem. B* **2010**, *114*, 9744−9750.
(60) Salvatierra, R. V.; Moura, L. G.; Oliveira, M. M.; Pimenta, M. A.; Zarbin, A. J. G. Resonant Raman Spectroscopy and Spectroelectrochemistry Characterization of Carbon Nanotubes/Polyaniline Thin Film Obtained through Interfacial Polymerization. *J. Raman Spectrosc.* **2012**, *43*, 1094−1100.

DOI: 10.1021/acsami.5b07459
ACS Appl. Mater. Interfaces 2015, 7, 24150−24158

(61) Ostrander, J. W.; Mamedov, A. A.; Kotov, N. A. Two Modes of Linear Layer-by-Layer Growth of Nanoparticle-Polylectrolyte Multilayers and Different Interactions in the Layer-by-Layer Deposition. *J. Am. Chem. Soc.* **2001**, *123*, 1101−1110.
(62) Lu, X. H.; Tan, C. Y.; Xu, J. W.; He, C. B. Thermal Degradation of Electrical Conductivity of Polyacrylic Acid Doped Polyaniline: Effect of Molecular Weight of the Dopants. *Synth. Met.* **2003**, *138*, 429−440.
(63) Cutler, C. A.; Bouguettaya, M.; Reynolds, J. R. PEDOT Polyelectrolyte Based Electrochromic Films via Electrostatic Adsorption. *Adv. Mater.* **2002**, *14*, 684−688.
(64) Li, Y.; Fu, Z. Y.; Su, B. L. Hierarchically Structured Porous Materials for Energy Conversion and Storage. *Adv. Funct. Mater.* **2012**, *22*, 4634−4667.
(65) Arico, A. S.; Bruce, P.; Scrosati, B.; Tarascon, J. M.; Van Schalkwijk, W. Nanostructured Materials for Advanced Energy Conversion and Storage Devices. *Nat. Mater.* **2005**, *4*, 366−377.
(66) Vetter, J.; Novak, P.; Wagner, M. R.; Veit, C.; Möller, K. C.; Besenhard, J. O.; Winter, M.; Wohlfahrt-Mehrens, M.; Vogler, C.; Hammouche, A. Ageing Mechanisms in Lithium-Ion Batteries. *J. Power Sources* **2005**, *147*, 269−281.
(67) Yoo, J. E.; Lee, K. S.; Garcia, A.; Tarver, J.; Gomez, E. D.; Baldwin, K.; Sun, Y. M.; Meng, H.; Nguyen, T. Q.; Loo, Y. L. Directly Patternable, Highly Conducting Polymers for Broad Applications in Organic Electronics. *Proc. Natl. Acad. Sci. U. S. A.* **2010**, *107*, 5712−5717.

DOI: 10.1021/acsami.5b07459
ACS Appl. Mater. Interfaces 2015, 7, 24150−24158